

## Flow boiling of ethanol/water binary mixture in a square microchannel

Parthenopi Vasileiadou<sup>1\*</sup>, Khellil Sefiane<sup>1</sup>, Tassos G. Karayiannis<sup>2</sup>

<sup>1</sup>School of Engineering, University of Edinburgh, The King's Buildings, Mayfield Road, Edinburgh EH9 3JL, UK

<sup>2</sup>College of Engineering, Design and Physical Sciences, Brunel University, London, Uxbridge UB8 3PH, UK

**Abstract:** Two-phase flow heat transfer was examined in a single 5mm inner hydraulic diameter square channel at a vertical orientation. Ethanol, deionized water and 5% v/v ethanol/water mixture were used as working fluids. Three mass fluxes (0.33, 0.66 and 1.00 kg/m<sup>2</sup>s) were tested as well as three heat fluxes (2.8, 4.2 and 6.1 kW/m<sup>2</sup>). Experiments were conducted in a controlled temperature environment (40°C) and high speed imaging, channel wall temperatures and local heat transfer coefficients were examined. The addition of ethanol into water (5% v/v ethanol/water mixture) was found to enhance heat transfer resulting in higher heat transfer coefficients than both of its pure components.

**Keywords:** flow boiling, heat transfer, micro-channel

### 1. Introduction

Several studies have been carried out over the past few years focusing on two-phase flow heat transfer in the microscale, which was suggested to induce increased heat transfer efficiency comparing to single-phase flow. Hence this type of heat transfer could be expected to serve as a competent cooling mechanism. In the electronics sector, progress created a requirement for increased cooling efficiencies. Other microsystems such as Micro-Electro-Mechanical Systems (MEMS), micro chemical reactors and compact heat exchangers would also be benefited from enhanced heat transfer in the microscale. Thus in this study focus was put on understanding and identifying the controlling mechanisms of two-phase flow heat transfer in microscale.

As reported by various studies, several factors were found to affect the heat transfer of a micro-cooling system. The main factors recognised were: the hydraulic diameter of the channels used (Yan and Lin <sup>1</sup>, Owhaib et al. <sup>2</sup>), their geometry (Tran et al. <sup>3</sup>) as well as the mass flux and the heat flux applied to the system. Moreover, the working fluid itself was found to be a determining factor in the heat transfer ability of a micro-system. A significant portion of research had been focused on different refrigerants, water and organic fluids. The thermophysical properties of an operating fluid were suggested to be an important factor in heat transfer, since in microscale surface tension and capillary forces are believed to influence heat transfer crucially (Thome <sup>4</sup>). Furthermore, latent heat of vaporisation and fluid viscosity were indicated to have a significant role in microscale flow boiling, according to Peng et al. <sup>5</sup>. That remark suggested that the liquids with higher liquid to vapour density ratio, greater thermal diffusion coefficients and larger latent heat demanded higher heat flux for the initiation of nucleation. After the onset of nucleation, liquids that have lower surface tension and lower latent heat of vaporisation induced higher heat transfer coefficients as stated by Greco and Vanoli <sup>6</sup>.

---

\* **Corresponding author:** Parthenopi Vasileiadou, Email: p.vasileiadou@ed.ac.uk

In the past decades, refrigerants were the fluids mainly used for cooling purposes. However, the impact of these fluids on the environment has been identified in recent times and hence, replacement liquids with similar heat transfer efficiencies needed to be found. The use of mixtures was one of the alternatives for the choice of a liquid that could be competent to the refrigerants. Miscellaneous multi-component mixtures were used as working fluids in studies in order to determine the potential increase in heat transfer in micro-scale comparing to their pure components or other pure liquids.

Binary mixtures of water with 2-propanol and methanol were examined by McGillis et al. <sup>7</sup> under pool boiling conditions and the critical heat flux (CHF) achieved for the mixture, at low alcohol concentrations, was found to be significantly higher than that of pure water. Fu et al. <sup>8</sup> experimented using ethanol/water mixtures in a diverging microchannel with microcavities. Their study showed that two-phase flow heat transfer coefficient was strongly dependant on the molar fraction of the mixture, as well as on wall superheat. Moreover, they concluded that addition of ethanol into water significantly increased the CHF recorded with the maximum CHF being achieved for a 0.1 ethanol molar fraction. More specifically, CHF of a 10% ethanol/water mixture was found to be 110% that of pure water, and 234% that of pure ethanol. This increase in CHF was considered to be a result of Marangoni effect being activated due to the addition of ethanol.

Mixtures of water with ethanol, propanol and butanol were examined by Suzuki et al. <sup>9</sup> in a subcooled flow boiling system to determine the effect that the addition of an organic fluid into water would have to heat transfer. It was observed that the maximum heat flux of the system increased with the addition of the organic fluid and no dry-out was recorded in that case. The maximum heat flux was found to be about 10% higher for the 10 wt% ethanol/water mixture comparing to that for pure water.

In this study, new aspects of flow boiling heat transfer will be examined for a 5% v/v ethanol/water mixture and its pure components (ethanol, water). The heat transfer coefficients of the three fluids will be determined in order to investigate the effect that the addition of ethanol in water has on heat transfer and whether it was enhanced compared to the pure fluids heat transfer. Also the behaviour of the two-phase flow heat transfer was visualised in high speed, to give a more complete view of the process.

## **2. Experimental apparatus and procedure**

### **2.1 Test section**

In this study a vertical square 5mm inner hydraulic diameter channel was used. The channel was manufactured with borosilicate glass and the outer surface was sputtered with tantalum, allowing the channel to become electrically conductive while remaining transparent. Heat was applied to the system using a power supply and electrodes, and at the same time the flow patterns within the channel were monitored with the use of a high speed camera. The thickness of the channel was 0.7mm and the test section heated length was 72mm. The working fluids used for the experiments were a 5% v/v ethanol/water mixture and its pure components: deionised water and ethanol.

### **2.2 Experimental setup**

The experimental setup consisted of a syringe pump that supplied the liquid to the channel and a DC power supply that provided the necessary power to heat up the system, through electrodes. The experiments were conducted in a 1m<sup>3</sup> (1×1×1 m<sup>3</sup>)

Plexiglas box which allowed for the control of the ambient temperature and hence, the minimisation of heat losses to the environment. The temperature was controlled by a PID controller mounted on the top of the Plexiglas box (Figure 1).

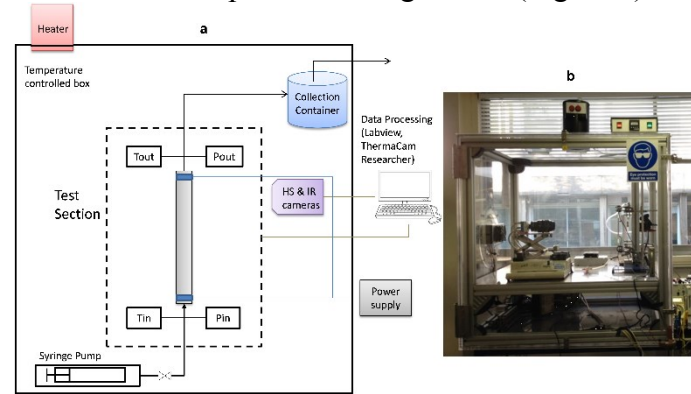


Figure 1. Experimental setup (a) schematic diagram, (b) picture (showing the Plexiglas box and the equipment)

The temperatures at the inlet and outlet of the channel were measured and recorded by two K type thermocouples and the PID controller was connected with a third same type thermocouple that was positioned inside the box. The data were recorded over time using National Instruments<sup>®</sup> software and a data acquisition device. A Mikrotron MC1310 high speed camera (set at 500 fps) and a Thermovision<sup>®</sup> 900 infrared (IR) camera (6 fps) were simultaneously recording the flowing patterns within the channel and the temperature profile of the outer channel wall. Experiments were conducted with three mass fluxes (0.33 kg/m<sup>2</sup> s, 0.66 kg/m<sup>2</sup> s and 1.00 kg/m<sup>2</sup> s) and three heat fluxes (2.8 kW/m<sup>2</sup>, 4.2 kW/m<sup>2</sup> and 6.1 kW/m<sup>2</sup>) for all the working fluids. The inlet temperature of the fluid was maintained constantly at 40°C and the surrounding pressure was 1atm. Thus, the subcooling temperature for each fluid was different: 60.0°C for water, 77.4°C for ethanol and 54.0°C for the 5% v/v ethanol/water mixture.

### 3. Data reduction

The data obtained from the measurements were used for calculating the local heat transfer coefficient and pressure drop along the channel according to the following order and equations.

#### 3.1. Heat losses

The power supplied to the system ( $Q_{sup}$ ) was computed using the voltage (V) and current (I) applied to the channel, using the equation:  $Q_{sup} = VI$ . (1)

For single-phase flow, the effective heat transferred to the liquid ( $Q_{eff}$ ):

$$Q_{eff} = \dot{m}c_{p,L}(T_{out,avg} - T_{avg}) \quad (2)$$

where  $\dot{m}$  is the mass flux (kg/s),  $c_{p,L}$  is the specific heat capacity of the liquid (J/kg K),  $T_{in,avg}$  and  $T_{out,avg}$  are the inlet and outlet temperatures respectively (averaged over time).

$$\text{The heat flux was then calculated as } q = Q_{eff}/A_{w,in} \text{ (kW/m}^2\text{)} \quad (3)$$

where  $A_{w,in}$  was the inner channel wall surface area (m<sup>2</sup>).

For two-phase flow in the channel, the effective heat applied ( $Q_{eff}$ ) on the channel section was:  $Q_{eff} = Q_{eff} - Q_{conv} - Q_{rad}$  (4)

Where  $Q_{conv}$  and  $Q_{rad}$  are the convective and radiative heat losses respectively.

<b>Table 1. Main uncertainties</b>		Convective heat loss was calculated by the following equation: $Q_{conv} = h_{conv}A_{w,out}(T_{w,avg} - T_{box})$ (5) where $h_{conv}$ is the convective heat transfer coefficient of air and it is estimated with the use of empirical correlations for natural convection. $A_{w,out}$ is the outer channel wall surface area, $T_{w,avg}$ the average wall temperature over time, for the overall channel surface, and $T_{box}$ is environment temperature. The radiative heat loss was then calculated from: $Q_{rad} = \varepsilon\omega A_{w,out}(T_{w,avg}^4 - T_{box}^4)$ (6) where $\varepsilon$ is the emissivity of the microchannel deposit and $\omega$ is the Stefan-Boltzmann constant ( $5.6703 \times 10^{-8} \text{ W/m}^2\text{K}^4$ ). The emissivity of the channel wall was experimentally estimated to be 0.78.
Parameter	Uncertainty (%)	
Pressure	$\pm 0.2$	
Pump volumetric velocity	$\pm 0.5$	
Voltage	$\pm 0.8$	
Current	$\pm 0.8$	
IR camera temperature	$\pm 1$	
Mass flux	$\pm 10.3$	
Heat flux	$\pm 7.3$	
Pressure drop	$\pm 0.5$	
Heat transfer coefficient	$\pm 20$	

### 3.2 Heat transfer coefficient

Infrared images of the top 2.8cm of the channel were recorded and hence, the wall temperatures and local heat transfer coefficients were obtained. The top part of the channel was analysed since boiling was present at that part of the channel for all the cases where two-phase flow was achieved and for all the fluids. The Biot number (Bi) was calculated to identify the temperature within the channel, comparing the conduction resistance to the convection resistance. The equation used to calculate the Biot number was:  $Bi = \frac{h_c \delta_{wall}}{k_{glass}}$  (7)

where  $h_c$  is the convective heat transfer coefficient calculated from the Shah and London<sup>10</sup> correlation for fully developed laminar flow with uniform heat flux at the wall, in a square channel.  $\delta_{wall}$  is the channel thickness and  $k_{glass}$  is the channel thermal conductivity. The Biot number was 0.035 and since  $Bi \ll 1$ , the difference between the inner and outer surface temperature could be neglected. Thus, the outer channel wall temperature could be used to calculate the local heat transfer coefficient  $h_L$ :

$$h_L = \frac{q_{eff}}{T_{w,local} - T_{sat}} \quad (8)$$

where  $T_{w,local}$  is the local wall temperature and  $T_{sat}$  is the saturation temperature of the working fluid. This equation was used when **two-phase flow** was present in the channel.  $T_{sat}$  for the pure fluids was calculated as a function of average (over time) inlet and outlet pressures. It was found that saturation temperature only changed by 0.5°C ( $\pm 1\%$ ) across the channel length. Hence, a steady saturation temperature was used for all the locations of the channel (average of inlet and outlet). For the 5% v/v ethanol/water mixture a similar behaviour was assumed, in lack of extensive vapour-liquid equilibrium data. The main uncertainties in measurements and calculated results are presented in Table 1.

In **single-phase** flow, local heat transfer coefficients were calculated using the following equation:  $h_L = \frac{q_{eff}}{T_{w,local} - T_{l,local}}$  (9)

where  $T_{l,local}$  is the local liquid temperature.

## 4. Results and discussion

### 4.1. High speed visualization results

In this set of experiments the liquid entered subcooled at the bottom of the channel at the same inlet temperature (40°C). Boiling started further along the length of the channel and, since subcooling and properties for each fluid were different, nucleation position was also different for each fluid for the same operating conditions.

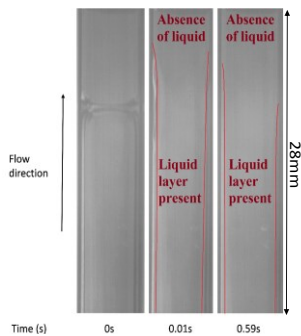


Figure 2. Ethanol boiling at  $G=0.33\text{kg/m}^2\text{s}$  and  $q=6.1\text{kW/m}^2$ , top 2.8cm of the channel length

Ethanol was found to be the fluid for which a lower amount of heat was required to induce boiling, which would be expected in accordance with its properties. Moreover, it was observed that bubble nucleation was more easily initiated for the ethanol/water mixture than for pure water, suggesting that the addition of alcohol in water (5% v/v) influenced the properties of the mixture significantly. Boiling was also found to be more vigorous in the case of ethanol and the ethanol/water mixture. When mass flux was decreased and heat flux was increased, there was dry-out observed at the top of the channel, as it can be seen in Figure 2 for ethanol. Dry-out was also observed for water at  $0.33\text{kg/m}^2\text{s}$  and

$6.1\text{kW/m}^2$  but not for the mixture. The lack of dry-out for the mixture suggested a more reliable heat transfer mechanism.

The boiling patterns observed varied depending on the operating conditions and the working fluid, while the main patterns recorded were bubbly, slug and elongated slug/annular flow (Figure 3) and they are in agreement with previous studies such as Huh and Kim<sup>11</sup> and Mishima and Hibiki<sup>12</sup>. Repeated recoiling and rewetting, or ebullition cycle as referred to by Carey<sup>13</sup>, is the mechanism that allows heat of vaporisation of the liquid to be used as a heat transfer mechanism and possibly increase the heat transfer efficiency of two-phase flow comparing to single-phase flow.

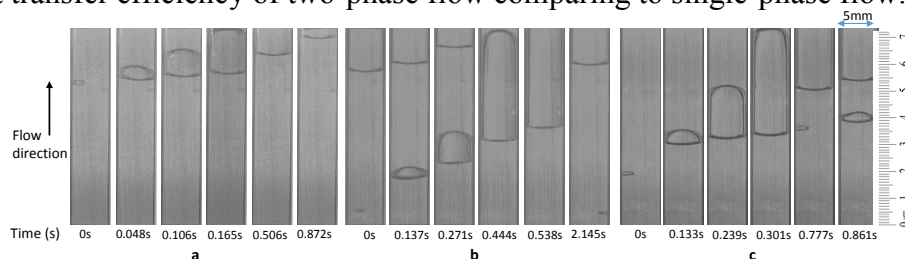


Figure 3. Flow regimes of boiling at  $G=0.33\text{kg/m}^2\text{s}$  and  $4.2\text{kW/m}^2$  for (a) water, (b) ethanol and (c) 5% v/v ethanol/water mixture, all the test section (7.2cm) is featured.

### 4.2. $T_w$ fluctuations for the different fluids

The temperature profile of the top 2.8cm of the channel outer wall was recorded with the IR camera at 6fps and temperature fluctuations over time were observed, which are believed to be the result of boiling in the channel. Only part of the channel was thermally mapped due to limited field of view and focus distance of the IR camera. The wall temperature ( $T_{\text{wall}}$ ) data at five positions at the top of the channel (Figure 4) were analysed.

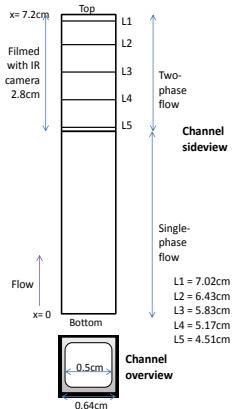


Figure 4. Schematic diagram of local heat transfer coefficients positions on the channel

seen that the temperature increased when the channel was filled with vapour and it decreased when liquid was covering the channel.

Comparing the wall temperature for the different fluids (Figure 6), it can be seen that wall temperature was the lowest for ethanol. In the case of the mixture however, it was seen that temperature fluctuations were substantially smaller, almost insignificant. Water was the fluid for which the wall temperature was the highest, especially in the cases of the highest heat flux.

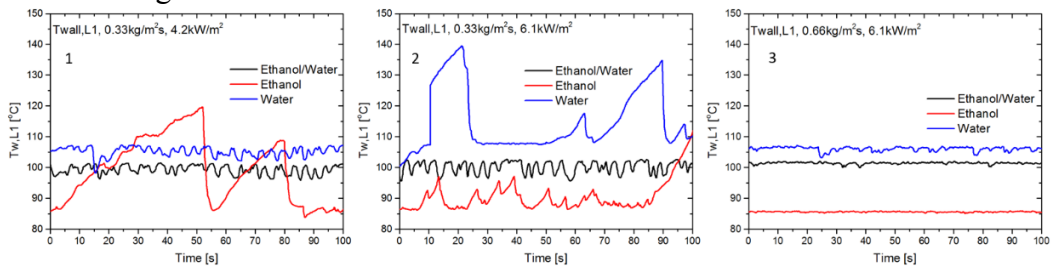


Figure 6. Channel wall temperature fluctuation at (1)  $G=0.33\text{kg/m}^2\text{s}$ ,  $q=4.2\text{kW/m}^2$ , (2)  $G=0.33\text{kg/m}^2\text{s}$ ,  $6.1\text{kW/m}^2$  and (3)  $G=0.66\text{kg/m}^2\text{s}$ ,  $q=6.1\text{kW/m}^2$ , at L1

### 4.3 Local heat transfer coefficients

Local heat transfer coefficients were calculated as a function of time for five positions at the upper section of the channel (Figure 4). It was concluded from the experiments that the higher heat transfer coefficients were for the ethanol/water mixture comparing to its pure components, ethanol and water, at the same conditions. Higher heat transfer coefficients were observed in the cases of two-phase flow and the highest ones were noticed for the cases with the lowest mass flux and highest heat flux (Figure 7).

Examining the calculated local heat transfer coefficients in synchronisation with high speed imaging, it was observed that higher  $h_L$  values were obtained when slug/annular flow was present in the channel, as opposed to bubble flow being present. Thus it could

From the results, it was concluded that when the system was at single-phase or where boiling had not commenced, the wall temperature was locally constant over. The temperature increased along the length of the channel, from the inlet towards the outlet of the channel. Conversely, during two-phase flow, fluctuations of wall temperature were noticed. Given that the heat was uniformly applied on the channel, it could be suggested that these fluctuations were entirely a result of boiling. The aforementioned phenomena can be observed in Figure 5, where until a certain length along the channel ( $x=60.7\text{mm}$ ) there is no boiling present and hence, there are no fluctuations in the wall temperature, while further along the channel temperature starts fluctuating. It could be implied that the fluctuations of temperature were a result of the alternating boiling regimes within the channel (vapour occupying channel followed by rewetting). It was

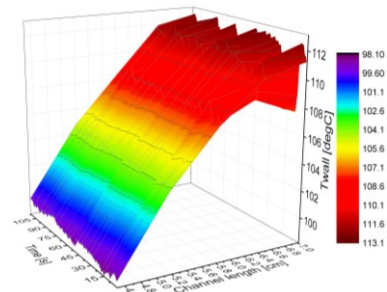


Figure 5. A 3-D plot of wall temperature against channel length and time for water at  $G=1.00\text{kg/m}^2\text{s}$ ,  $q=6.1\text{kW/m}^2$



be suggested that in those cases another heat transfer mechanism was activated, i.e. the liquid film evaporation, working along with forced convection.

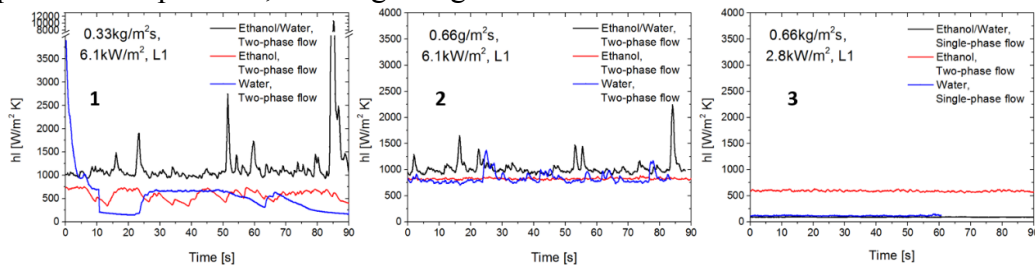


Figure 7. Local heat transfer coefficient over time of 5% v/v ethanol/water mixture, water and ethanol for (1)  $G=0.33\text{kg/m}^2\text{s}$ ,  $q=6.1\text{kW/m}^2$ , (2)  $G=0.66\text{kg/m}^2\text{s}$ ,  $q=6.1\text{kW/m}^2$ , (3)  $G=0.66\text{kg/m}^2\text{s}$ ,  $q=2.8\text{kW/m}^2$

Averaged local heat transfer coefficients over time were also calculated to allow for a numerical comparison between the different fluids. The average local heat transfer coefficients at the lowest mass flux and highest heat flux ( $0.33\text{kg/m}^2\text{s}$  and  $6.1\text{kW/m}^2$ ) at position L1 were:  $420\text{W/m}^2\text{K}$  for ethanol,  $540\text{W/m}^2\text{K}$  for water and  $1200\text{W/m}^2\text{K}$  for the ethanol/water mixture (three times higher than that of ethanol and roughly twice as much as the water value). However, in the case of the highest mass and heat flux ( $1.00\text{kg/m}^2\text{s}$  and  $6.1\text{kW/m}^2$ ), ethanol and ethanol/water mixture  $h_L$  values were closer together;  $940\text{W/m}^2\text{K}$  for ethanol/water and  $860\text{W/m}^2\text{K}$  for ethanol. The  $h_L$  value for water was substantially lower ( $460\text{W/m}^2\text{K}$ ). The heat transfer coefficients values for the fluids were closer together when mass flux was increased and, given the uncertainty of the calculated values ( $\pm 20\%$ ), it was not possible to distinguish which fluid was more heat transfer efficient at higher mass fluxes.

Finally, it was noticed that higher heat transfer coefficients could be achieved for the mixture, while avoiding a possible dry-out. The ethanol/water mixture is a positive mixture, for which boiling/evaporation occurs at different rates for each component (more volatile component evaporates first). Hence, a concentration gradient occurs, which leads to Marangoni forces being induced and in turn, to bulk liquid movement towards the contact line (Fu et al. <sup>8</sup>). This behaviour results in a better liquid distribution in the channel, which helps prevent dry-out from happening.

## 5. Conclusions

In this study different aspects of two-phase flow heat transfer for a 5% v/v ethanol/water mixture and its pure components (water and ethanol) were investigated. High speed imaging of boiling was obtained along with the channel wall temperature and local heat transfer coefficients were calculated.

Several boiling patterns were identified, using high speed visualisation, which varied depending on the operating conditions of the experiment. The boiling regimes observed were: bubble, slug and elongated slug/annular flow.

The channel wall temperature profile was also recorded over time and it was analysed to determine the effect boiling had on it and, more specifically, how different boiling regimes influenced its fluctuations. It was concluded that channel wall temperature fluctuated over time with two-phase flow, and that this was solely a result of boiling occurring in the channel. Ethanol was recognised as the fluid that was able to maintain the wall temperature at the lowest levels, with ethanol/water mixture following. However, it was seen that the ethanol/water mixture significantly decreased the

amplitude of fluctuations occurring during boiling, allowing for a more stable heat transfer process over time.

Lastly, heat transfer was enhanced by the addition of ethanol into water, resulting in higher heat transfer coefficients than both of its pure components. The heat transfer coefficients fluctuations (over time) were compared to high speed imaging. The reverse flow of liquid followed by the rewetting of the channel walls (slug passing through channel) was found to increase heat transfer efficiency. Finally, the use of the mixture ensured the prevention of wall dry-out, which could lead to a potential critical failure in a cooling system.

### Acknowledgements

This research was supported by the UK Engineering and Physical Sciences Research Council (EPSRC) grant EP/N011341/1.

### References

1. Yan, Y. Y. & Lin, T. F. Condensation heat transfer and pressure drop of refrigerant R-134a in a small pipe. *Int. J. Heat Mass Transf.* **42**, 697–708 (1999).
2. Owhaib, W., Martín-Callizo, C. & Palm, B. Evaporative heat transfer in vertical circular microchannels. *Appl. Therm. Eng.* **24**, 1241–1253 (2004).
3. Tran, T. N., Wambsganss, M. W. & France, D. M. Small circular- and rectangular-channel boiling with two refrigerants. *Int. J. Multiph. Flow* **22**, 485–498 (1996).
4. Thome, J. R. State-of-the-Art Overview of Boiling and Two-Phase Flows in Microchannels. *Heat Transf. Eng.* **27**, 4–19 (2006).
5. Peng, X. F., Hu, H. Y. & Wang, B. X. Boiling nucleation during liquid flow in microchannels Liquid # Vapor ~ N ~ Liquid bubble. *Science (80-. )*. **41**, (1998).
6. Greco, a. & Vanoli, G. P. Flow boiling heat transfer with HFC mixtures in a smooth horizontal tube. Part I: Experimental investigations. *Exp. Therm. Fluid Sci.* **29**, 189–198 (2005).
7. McGillis, W. R., Fitch, J. S., Hamburg, W. R. & Carey, V. P. WRL Technical Note TN-23 Boiling Binary Mixtures at Subatmospheric Pressures. (1999).
8. Fu, B. R., Tsou, M. S. & Pan, C. Boiling heat transfer and critical heat flux of ethanol-water mixtures flowing through a diverging microchannel with artificial cavities. *Int. J. Heat Mass Transf.* **55**, 1807–1814 (2012).
9. Suzuki, K. *et al.* Enhancement of heat transfer in subcooled flow boiling with microbubble emission. *Exp. Therm. Fluid Sci.* **29**, 827–832 (2005).
10. Shah, R. K. & London, A. L. *Laminar flow forced convection in ducts: a source book for compact heat exchanger analytical data*. **1**, (Academic press, 2014).
11. Huh, C. & Kim, M. H. Pressure Drop, Boiling Heat Transfer and Flow Patterns during Flow Boiling in a Single Microchannel. *Heat Transf. Eng.* **28**, 730–737 (2007).
12. Mishima, K. & Hibiki, T. Some characteristics of air-water two-phase flow in small diameter vertical tubes. *Int. J. Multiph. Flow* **22**, 703–712 (1996).
13. Carey, V. P. *Heterogeneous nucleation and bubble growth in liquids. Liquid-Vapor Phase-Change Phenomena: An Introduction to the Thermophysics of Vaporization and Condensation Processes in Heat Transfer Equipment*. (Taylor & Francis, 2008).
14. Bertsch, S. S., Groll, E. a. & Garimella, S. V. Effects of heat flux, mass flux, vapor quality, and saturation temperature on flow boiling heat transfer in microchannels. *Int. J. Multiph. Flow* **35**, 142–154 (2009).